Simple and efficient software-based stabilized holographic recording system

George Cadena
Omid Momtahan
Ali Adibi, MEMBER SPIE
Georgia Institute of Technology
School of Electrical and Computer Engineering
Atlanta, Georgia 30332-0250
E-mail: adibi@ee.gatech.edu

Abstract. A simple, inexpensive, and efficient stabilized holographic recording setup is described which precludes the destructive fringe movement encountered in long-lasting holographic exposures. Utilizing a straightforward methodology, stability greater than $\lambda/25$ (recording wavelength $\lambda=532$ nm) for holographic recording sessions longer than 6 h can be achieved. Due to the software basis of this design, in the LabVIEW platform, the functionality of expensive hardware components is provided in software. Moreover, this setup is modularly designed and can be easily replicated for multiple labs, with the need only of the following hardware components: a piezo-shifting mirror, a computer, a data-acquisition card, and a photodetector. [DOI: 10.1117/1.2403089]

Subject terms: holographic recording; stabilizer system.

Paper 050996R received Dec. 25, 2005; revised manuscript received May 12, 2006; accepted for publication May 22, 2006; published online Jan. 2, 2007.

1 Introduction

As technological innovations make expensive and large experimental setups more compact and affordable, applications involving holographic interferometry become more and more practical and realizable. The principle of holographic interferometry is straightforward: two coherent optical beams—an information-bearing signal beam and a reference beam—are superimposed in a photosensitive material.[1] The interference of these two beams produces a fringe pattern, a beam of light with a spatially varying intensity. The modulated intensity pattern is recorded as a change in optical properties of the photosensitive material forming a grating or a hologram.[2,3] The intensity pattern can modify the absorption of the material and record an amplitude grating, can modulate the refractive index of the medium and form a phase grating, and/or can be a combination of both processes. On reading with the reference beam, a beam exactly similar to the recording signal beam diffracts from the hologram. The ratio of the intensity of this diffracted beam to the intensity of the reading reference beam is called the diffraction efficiency of the hologram.

Successful recording of the grating strongly depends on the stability of the recording setup during the change in the properties of the photosensitive material, especially when long exposure is required. Outside influences such as mechanical vibrations or perturbations due to airflow will cause movement in the optical beam path that modifies the spatial index modulation and directly affects the strength of the grating. This limitation becomes more evident when attempting long holographic exposures; therefore, an active stabilizer is an essential component in the production of strong gratings.[4]

The basic operation of an active stabilizer is to monitor any movement in the fringe pattern (as shown in Fig. 1) during a holographic recording session and compensate that movement by shifting one of the recording beams. It is evident that the stability is in proportion to the precision of the measurement and the accuracy of the compensation; thus, eliminating background noise is a key factor for stabilization. Two such hardware components that satisfy the aforementioned requirements are a lock-in amplifier (LIA) and a piezo-shifting mirror (PZM).[5,6] A lock-in amplifier takes a periodic reference signal embedded in a noisy input and uses a phase-sensitive detector (PSD) to extract only that part of the output signal whose frequency and phase match the reference.[7] A PZM is used for ultrafine axial positioning and for modulation of the reference signal at high resonance frequencies with submicron resolution.[8] The combination of these two components into an interferometric setup allows for the ability to modulate a fringe pattern with minute amplitude, negligible throughout the recording session, and—through beam coupling—extract the developing diffracted beam to stabilize the setup.[9] Dis-

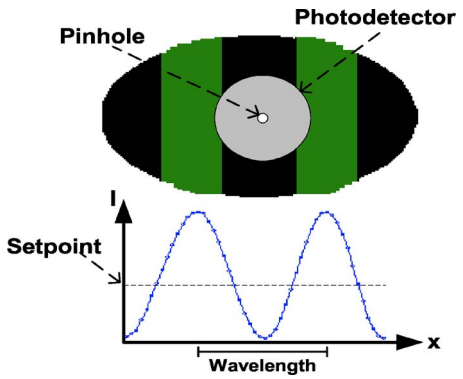

Fig. 1 Illustration of a photodetector, with a pinhole, placed in the path of a magnified interference pattern. The reading from the photodetector is the process variable. The graph of intensity (I) versus distance (x) displays the quantitative position of the set point in relation to the intensity pattern.

0091-3286/2006/$22.00

advantages of this implementation are its experiment-specific properties and the high costs of hardware components such as the PZM, LIA, function generator, and integrator.

In this paper, we present a simple and cost-effective approach to active stabilization that provides results comparable to those found in conventional hardware-based setups. The primary advantage of the proposed software-based technique is the replacement of the functionality of the previously mentioned hardware devices with the signal-processing capabilities of the LabVIEW software[10,11] that is available in almost all optics labs.

2 Methodology

The stabilization scheme is as follows: an interference pattern is formed by splitting a coherent laser beam into two parts of equal intensity and passing those parts into an interferometer (a Mach-Zender interferometer in our implementation). Section 4 describes the setup in more detail. The interference pattern is imaged onto a photodetector with a pinhole covering. The graph of intensity versus lateral distance in Fig. 1 illustrates the quantitative relationship between the set point and the interference pattern. The set point (further discussed in Sec. 5) is a value selected before the operation of the stabilizer and can correspond to any phase difference between the interfering beams. The reading from the photodetector is the process variable (PV), and is subtracted from the set point to produce an error. The error is then processed by a proportional-integral-derivative (PID) controller in series with another PID controller that has only integral gain.[12] Following this, the processed error is passed to a phase-shifting element, PZM, to compensate the phase perturbation in the fringe pattern, hence completing the closed loop.[13,14] The actual rate for repeating this process depends on the instability in the setup, and it can affect the final stability. For our case, we chose a rate of 40 Hz, which resulted in very good stability (less than $\lambda/25$).

A successful method for making a stable setup is to use PID controllers to compensate for the poles and zeros of the system. In our design, we follow and compensate for the poles and zeros by using a PID controller that utilizes proportional and integral gain. The derivative gain is either zero or very small, to reduce the oscillatory behavior. Adding another PID with only integral gain (which mainly acts as a memory) will allow us to not only compensate the changes but also track the sudden changes more accurately. Since the actual system functions for some of the elements (like the PZM) are not exactly known, the PIDs should be tuned in the actual stable system. The tuning methodology of the PID controllers is the most critical aspect of this stabilization setup. The determination of the first PID gain parameters is done according to the Ziegler-Nichols tuning method,[15] and fine tuning is done by trial and error. There is no tuning involved in the second PID controller, since only the integration function is used, and it is in series with the first PID controller. The versatility of our software-based approach allows for the simple implementation of multiple PID controllers, whereas the implementation of such a task in hardware is laborious and expensive.

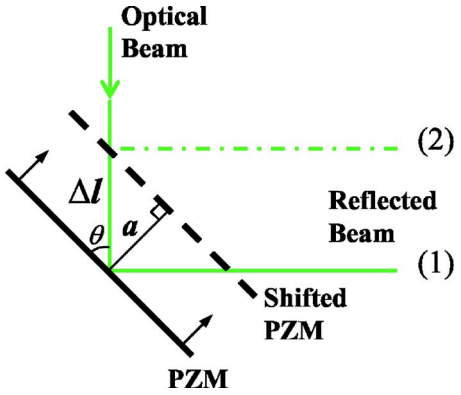

Fig. 2 Schematic of the shift of the PZM and the effect on the signal beam. Here Δl is the change in the beam path length, a is the shift of the mirror, θ is the angle between the beam and the PZM, (1) shows the reflected beam before shifting the PZM, and (2) shows the reflected beam after shifting the PZM.

3 Theory

The result of external perturbation of the holographic system is the movement of the fringe pattern at the plane of the photodetector (see Fig. 1). Focusing on the proportional relationship between the intensity I and the time average of E^2, the intensity equation is $I=A\langle E^2\rangle$, where $\langle\square\rangle$ represents time averaging and A is a constant. The interfering waves E_1 and E_2 both have the same frequency, and $E=E_1+E_2$. Assuming that the beams are in the (x,y) plane, the electric fields of the two interfering waves are defined as [13,16]

$$E_1 = A_1 \exp\{j[\omega t + \phi_1(x,y) + \delta_1(t)]\}, \tag{1}$$

$$E_2 = A_2 \exp\{j[\omega t + \phi_2(x,y) + \delta_2(t) + k\,\Delta l(t)]\}, \tag{2}$$

where E_1 corresponds to the reference beam and E_2 corresponds to the signal beam, which is adjusted by the PZM. Furthermore, A_1 and A_2 are field amplitudes, ω is the angular frequency, ϕ is the initial phase difference between the two light waves under perfectly stable conditions ($\phi=\phi_1-\phi_2$), $\delta_i(i=1,2)$ is the phase perturbation that arises from any change in the path length of the beam i, k is the propagation constant, and $\Delta l(t)$ is the path-length difference between the two waves. Assuming that both waves are linearly polarized and perfectly coherent, the interference pattern at the plane of the photodetector is

$$I = A_1^2 + A_2^2 + 2A_1A_2\cos[\phi(x,y) + \delta(t) - k\,\Delta l(t)], \tag{3}$$

where $\delta=\delta_1-\delta_2$ is the net perturbation of the relative phase. By placing a pinhole on the detector that is small compared with the period of the interference pattern, the unperturbed phase becomes constant, $\phi_0=\phi(x_0,y_0)$ with x_0 and y_0 being the coordinates of the pinhole, so that the only variables in the interference pattern are $\delta(t)$ and $\Delta l(t)$. The derivation of the path-length difference in terms of the mirror shift a can be seen in Fig. 2. Through geometric reasoning in Fig. 2, the change in the path length of the signal beam (Δl) due to shifting the PZM by a is $\Delta l=a/\sin\theta$, and for $\theta=45$ deg, we obtain $\Delta l=\sqrt{2}a$. Hence, the stabilization condition may be reduced to $|k\sqrt{2}\cdot a|=|\delta(t)|$. The minimum

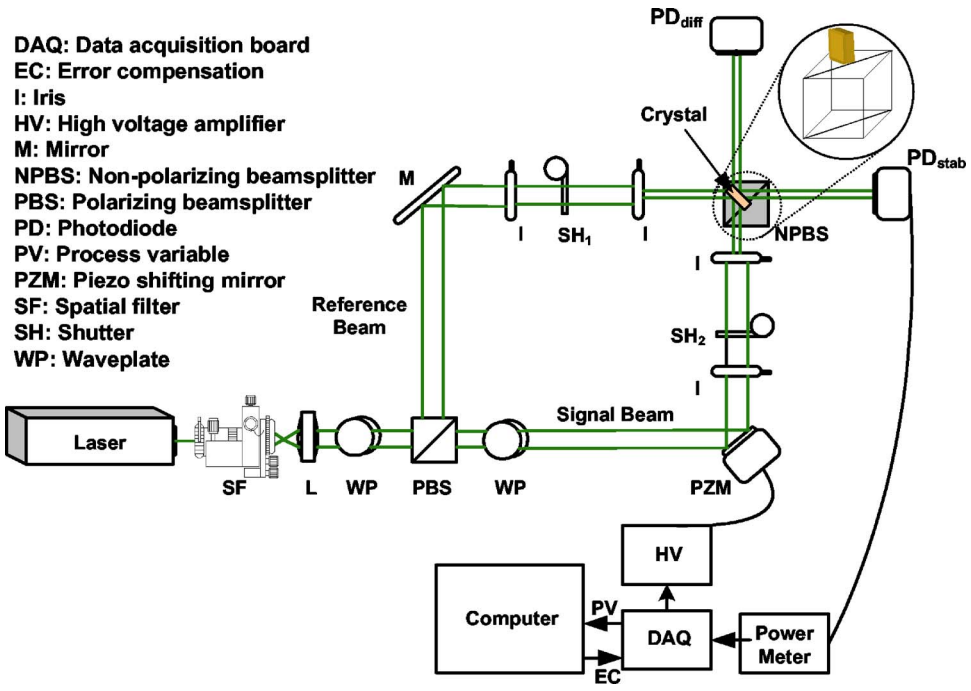

Fig. 3 A Mach-Zender interferometer stabilized by monitoring the movement of the interference pattern with a photodetector and a power meter. The movement of the interference pattern is represented as a voltage and is sent through a DAQ card into a computer as a process variable (PV), which is then processed in software and returned as an error-compensation (EC) value through a DAQ card to the PZM through a high-voltage amplifier. Note that the holographic recording material (crystal) is mounted on top of the beamsplitter (NPBS).

shift for our mirror is $a=\lambda/100$ for $\lambda=532$ nm. Therefore the minimum path length that this setup may compensate for is $\sqrt{2}\lambda/100$.

4 Holographic Setup

The setup in Fig. 3 consists of two parts. The first part, which is based on Mach-Zender interferometry, is primarily used for stabilization.[6,9] The other part is used for recording the holograms in transmission geometry independent of the recording material. Note that these two parts are implemented using the same beams by placing the recording material (crystal) on top of the nonpolarizing beamsplitter (NPBS) as shown in Fig. 3.

A continuous-wave solid-state laser generates light at $\lambda=532$ nm. The beam is spatially filtered, expanded, collimated, and split into two beams. If the cross sections of the split beams are not large enough to encompass both the crystal and the beamsplitter (NPBS), extra lenses (not shown in Fig. 3) should be used to expand the beams. The lower portion of the signal beam is partially reflected by the nonpolarizing beamsplitter and overlaps with the partially transmitted reference beam. Since these two beams are collinear, large fringes can be formed at the photodetector, PD_{diff}. The crystal is placed on the top of the beamsplitter as shown in the inset of Fig. 3. The upper portions of the reference and signal beams overlap and form an interference pattern inside the crystal to record the hologram.

A PZM is placed in the path of the signal beam. Irises are used for alignment and to adjust the size of the beams that reach the crystal. The shutters, controlled in LabVIEW, are used for holographic recording and readout only. A photodetector, PD_{diff}, is placed in the signal beam path, aligned with the height of the crystal, to measure the intensity of the diffracted light during read out. The photodetector, PD_{stab}, placed in the reference beam path, is aligned below the crystal but in line with the beamsplitter to monitor fringe movement. An extra lens might be used in front of PD_{stab} to magnify the image of the fringes on the detector. A pinhole covering is placed in front of PD_{stab}. The size of the pinhole with respect to the fringe spacing should be small enough to measure a fringe movement of $\lambda/50$. The fringe spacing depends on the alignment of the two beams after the NPBS, which can be adjusted by varying the position of the beam splitter.

It should be noted that the performance of the stabilizer depends on the accurate detection of the fringe movement, which depends in part a on the diameter of the pinhole, the resolution of the detector, and the noise power at the detector. If the small change in the detected power corresponding to the fringe movement is less than the resolution of the detector or is comparable to the noise power, the fringe movement will not be detected correctly and the stability of the system will be less.

The fringe movement recorded by PD_{stab} is taken into the computer via a data acquisition card (DAQ) and processed in LabVIEW, where a phase compensation voltage is determined and sent to a high-voltage amplifier, which controls the motion of the PZM. To obtain a large contrast for the fringes and a large modulation depth for holographic recording, the intensities of the two beams should be the same. The first half-wave plate (WP1) is used to adjust the relative intensity of the reference and the signal

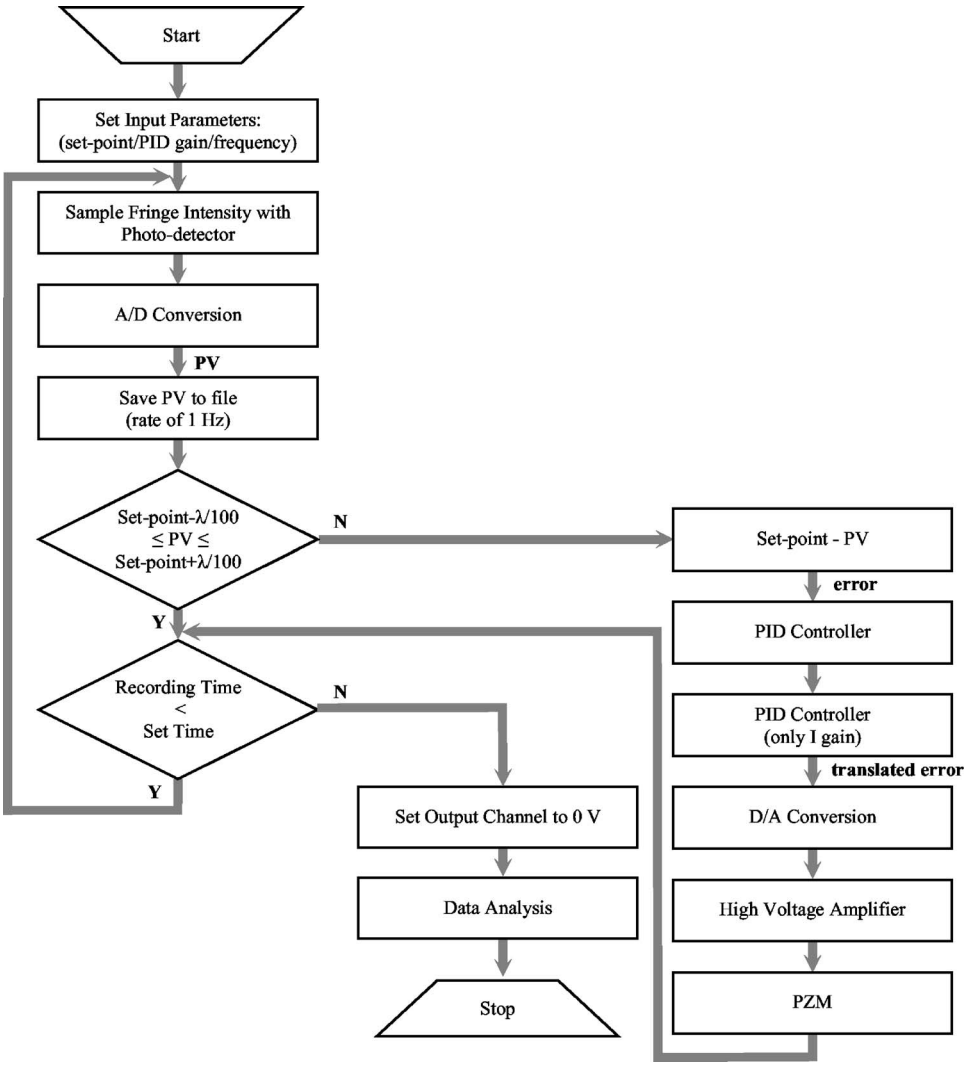

Fig. 4 Flow chart describing the stability algorithm.

beams. The second half-wave plate (WP2) is used to rotate the polarization of the signal beam and make it the same as that of the reference beam.

5 Software Basis

LabVIEW is an open environment that operates through a graphical language in which lines of code are replaced by block diagrams.[10,11] It comes equipped with an extensive library of ready-to-use programs that can replicate the functionality of most state-of-the-art hardware devices. In view of the versatility of this software platform, there is no justification for adding any other hardware components to our setup apart from the PZM. However, if one should desire to add a LIA for extracting the diffracted beam directly from the hologram, its functionality could be reproduced,[17] yet with potential limitation from the sampling rate of the data acquisition (DAQ) card.

The overall flow chart of the system process is shown in Fig. 4. The preliminary operations include inputting the set point, PID gain, and frequency. Since the full peak-to-peak range of the interference pattern is measured in analog form, its conversion to digital provides a numerically equivalent range. Selecting any number in that range corresponds to selecting a phase value between the two interfering beams. This initial selection is the set point for the stabilizer system. The frequency is the rate at which the stabilizer operates. The minimum frequency should be selected to compensate for all the instability disturbances. The maximum frequency is limited by the sampling rate of the DAQ or the delay in processing the data. In this work, the maximum achieved frequency was 100 Hz, while the full stabilization could be achieved with a frequency of 40 Hz. The PID gain parameters should be initially determined, as discussed in Sec. 2, and set in the software.

The process begins by reading and recording the intensity from the interference pattern. That value is converted to digital, averaged, and saved to a file at a rate of 1 Hz. The averaged data (PV) are then compared with a range that corresponds to the minimum mirror shift, $\lambda/100$, above and below the set point. If the PV is outside this range, an error value is determined and processed in successive PID controllers, the latter having only integral (I) gain. The translated error value corresponds to an error-compensating voltage, which is sent to the PZM. This process is repeated

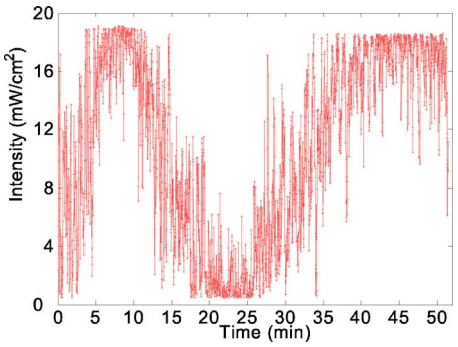

Fig. 5 Intensity monitored by photodetector (PD_{stab} in Fig. 3) over a 50-min interval without the operation of the active stabilizer.

as long as the operation time is less then the set time. Once the program terminates, a zero voltage is sent to the data acquisition card to clear any remaining voltage on the output channel, and a MATLAB script is run that analyzes and graphs the recorded data.

One of the main limitations of implementing a closed-loop control system (as explained here) in LabVIEW is the delay between sampling and sending the control signal. This delay might be from the data processing or from the lack of synchronization between the sample and the current state of the system. We have measured our processing time, and it is negligible compared to the sampling period. However, real-time sampling and controlling is found to be essential for achieving a stable setup. Since synchronization in LabVIEW is not easily achieved, it needs to be made explicit with a sequence structure, such that the response of each section of operation is taken into account (i.e., the data acquisition of the reading from the photodetector, the signal processing of the data, and the output of a control voltage to the PZM). This sequential implementation is the essence of the flow chart shown in Fig. 4.

6 Results

Figure 5 is a representation of the movement of the nonstabilized interference pattern without the operation of the active stabilizer over a period of 50 min while external sources, including the air conditioning, were off. Such erratic behavior may be attributed to vibration from laser cooling fans, shutters, motors, thermal gradients, air motion (both convective and random), ambient temperature changes, humidity changes, and aging optics.[14,18]

A primary application of this stabilization system is long-exposure holographic storage. One specific case is the investigation of two-center holographic recording, in which holograms are recorded over a long period of time.[19] The system stability in this case may be measured by monitoring the development of the diffraction efficiency. In addition, a complete record of the process variable (the reading from PD_{stab},) obtained during the recording session also proves to be informative. Figure 6(a) shows the variation of the output of PD_{stab} (corresponding to the intensity variation of the interference pattern) as a function of time when the PZM shifts linearly. The peak-to-peak range illustrated in Fig. 6(a) is the maximum amount that the fringe pattern may move if it is not stabilized. Fig. 6(b) illustrates the effect of the stabilization system in locking the movement of the fringe pattern to a set point, within that range, for a long period of time. The full range (peak to peak) of the interference intensity in Fig. 6(a), when interpreted through the DAQ card and software, produces the output 1.88 V. The two lines in the inset of Fig. 6(b) show the maximum range of the output when the stabilizer is running. The maximum range within the lines is about 0.15 V. The ratio of this maximum range to the full peak-to-peak range of the output of the interference intensity is about 1/12.5. Since the period of the interference pattern in Fig. 6(a) corresponds to one wavelength (λ), the peak-to-peak range corresponds to $\lambda/2$, and the resultant stability of $\lambda/25$ is obtained. The stabilizer was run for more than 6 h (380 min),

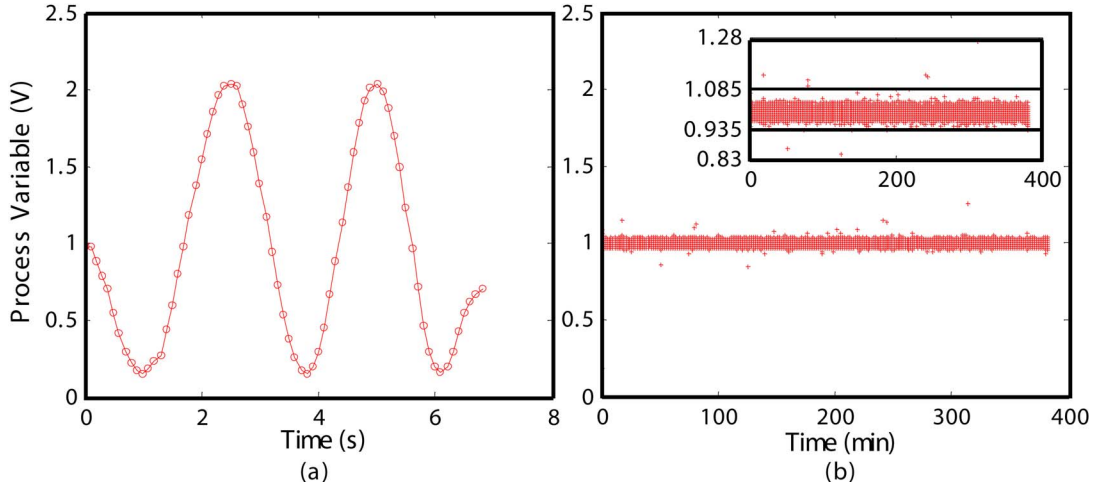

Fig. 6 Comparison of (a) the experimental measure of the full range of the intensity pattern obtained from PD_{stab} when the mirror shifts continuously with (b) the interference pattern stabilized for a period of 380 min. The two lines in the inset of (b) show the maximum range of the stable output. The maximum range within the lines is about 0.15 V.

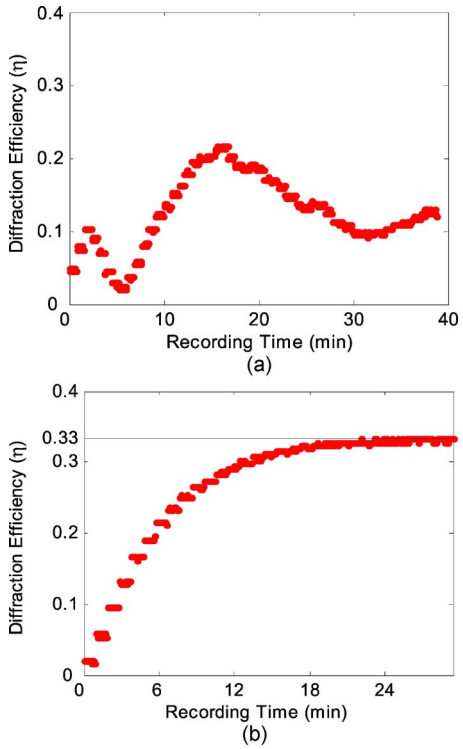

Fig. 7 Development of the grating as illustrated by the diffraction efficiency versus the recording time for a two-center hologram recoded in a 2-mm-thick $LiNbO_3$:Fe:Mn crystal (a) under nonstabilized conditions and (b) under stabilized conditions. The total recording beam intensity and the sensitizing intensity were 86 and 38 mW/cm^2, respectively, and the sensitization and recording wavelengths are 532 and 404 nm, respectively.

an amount of time that is more than sufficient for long-time holographic exposures, and we observed stability better than $\lambda/25$ over this entire interval.

To show the importance of using the stabilizer system for holographic recording, we performed two similar experiments with and without the operation of the stabilizer. For two-center holographic recording, a 2-mm-thick congruent $LiNbO_3$ crystal doped with 0.15 wt% Fe_2O_3 and 0.02 wt% MnO is first oxidized at 1070°C for 48 h in an oxygen environment and then placed in the setup with recording intensities I_{sig}=43 mW/cm^2 of the signal beam I_{ref}=43 mW/cm^2 of the reference beam. The two beams have ordinary polarization (i.e., the electric field is perpendicular to the plane of incidence) and the grating is formed in the direction of the c axis of the crystal. During the recording, the crystal is sensitized by a blue laser at wavelength λ=404 nm (not shown in Fig. 3). The intensity of the sensitizing beam is 38 mW/cm^2.

Figure 7 shows the development of the diffraction efficiency (with time) under stabilized and nonstabilized conditions. Under nonstabilized conditions [Fig. 7(a)], the hologram exhibits patterns of erasure and rerecording, which are an indication of the instability of the recording fringe pattern. In contrast, Fig. 7(b) illustrates continuous recording of the volume hologram to its saturation level, which is an indication of excellent fringe stability provided by the stabilizer. Thus, Fig. 7 clearly shows that the stabilizer cancels the instability over a long period of time.

7 Discussion

One of the major limitations of the digital approach to active stabilization has been its inferior performance in comparison with analog techniques. However, a high-quality data-acquisition card makes digital stabilization a viable alternative. In the software implementation of the stabilizer, we used a standard DAQ board with 12-bit resolution and a maximum sampling rate of 200 Hz. The temporal limitation of the stabilizer came from the sampling rate of this card. Eliminating all functions apart from those essential to stabilization, we were able to achieve stability at frequencies up to this rate. Although the result depends on the condition of our system and the long-time stability requirement, we found empirically that 40 Hz was the minimum sampling frequency to achieve $\lambda/25$ stability. Sampling at rates higher than 40 Hz provided no significant improvement. An additional system delay is from recording to file the information of the stabilizer (the reading from PD_{stab},) and the development of the diffraction efficiency (the reading from PD_{diff}). We found that saving this information at the rate of 40 Hz was unnecessary, since the movement of the fringe pattern in the nonstabilized system fluctuated over times on the order of a few seconds. We chose to record the behavior of the system and monitor the development of the diffraction efficiency at a rate of 1 Hz, while simultaneously stabilizing the system at a rate of 40 Hz.

The most significant limitation that arose in regard to the stability came from the resolution of the mirror. The maximum stability that it could achieve is approximately $\lambda/50$, which allows only two steps for the mirror to shift (one step forward and one backward from the initial position). We could achieve that high resolution for 30 min; details are not reported here.

The modular design we presented for the stabilizer can be used to run fully automated holographic recording experiments. It can also benefit from widely available built-in functionalities of LabVIEW. As an example, the experiment can be monitored and controlled remotely by accessing the LabVIEW front panel controls from a standard web browser. Also, the capability to log data at multiple stages of the process can be used for debugging and monitoring of very long experiments. Moreover, if problems arise, our software approach bypasses the arduous process of hardware repair.

8 Conclusion

Under holographic exposures longer than a few minutes, problems such as random air motion and fluctuations in the ambient temperature result in changes in the optical path length that severely degrade the strength of a grating.[14] Since disturbance in the optical path length can be detected in the form of phase variation and,[20] monitoring the phase variations of the interference pattern provides an accurate method to stabilize the holographic setup. We have reported here, for the first time to our knowledge, the implementation of this by a simple technique in software using LabVIEW. The software basis of this design greatly reduces the cost of the stabilized holographic recording setup at minimal compromise in system stability. Our setup provides an overall stability of $\lambda/25$ for a period of more than 6 h, at a significantly reduced cost compared to conventional

hardware-based setups. The only elements needed in our design are the computer, LabVIEW software, piezo shifting mirror, photodetector, and data acquisition card with analog-to-digital and digital-to-analog conversion. It should be mentioned that these elements, apart from the mirror, are available in almost all optical laboratories. Based on these relatively standard requirements and the ease of replication with software, it is conceivable that a software-based stabilizer may be placed in every lab that requires long-time holographic exposures with excellent stability at minimal cost.

Acknowledgments

This work was supported by the Air Force Office of Scientific Research under G. Pomrenke (Grant No. FA9550-05-1-0438). G. Cadena thanks Dr. Gary May and the SURE program at Georgia Tech for summer research support.

References

1. G. T. Sincerbox, "History and physical principles," in *Holographic Data Storage*, H. J. Coufal, D. Psaltis, and G. T. Sincerbox, Eds., pp. 3–20, Springer (2000).
2. F. S. Chen, J. T. LaMacchia, and D. B. Fraser, "Holographic storage in lithium niobate," *Appl. Phys. Lett.* **13**, 223–225 (1968).
3. W. S. Colburn and K. A. Haines, "Volume hologram formation in photopolymer materials," *Appl. Opt.* **10**, 1636–1641 (1971).
4. P. M. Garcia, K. Buse, D. Kip, and J. Frejlich, "Self-stabilized holographic recording in LiNbO3:Fe crystals," *Opt. Commun.* **117**, 235–240 (1995).
5. J. Frejlich, L. Cescato, and G. F. Mendes, "Analysis of an active stabilization system for a holographic setup," *Appl. Opt.* **27**, 1967–1976 (1988).
6. P. Acioly, M. Dos Santos, L. Cescato, and J. Frejlich, "Interference-term real-time measurement for self-stabilized two-wave mixing in photorefractive crystals," *Opt. Lett.* **13**, 1014–1016 (1988).
7. Stanford Research Systems, "About lock-in amplifiers," Application Note 3, http://www.thinksrs.com/downloads/PDFs/ApplicationNotes/AboutLIAs.pdf (1999).
8. Piezomechanik "Piezo-based optomechanics," Application Catalogue, http://www.piezomechanik.com (2003).
9. K. Peithmann, A. Wiebrock, and K. Buse, "Incremental holographic recording in lithium niobate with active phase locking," *Opt. Lett.* **23**, 1927–1929 (1998).
10. J. Y. Beyon, *LabVIEW Programming, Data Acquisition and Analysis*, Prentice Hall PTR (2001).
11. G. W. Johnson and R. Jennings, *LabVIEW Graphical Programming*, 3rd ed., McGraw-Hill, New York (2001).
12. B. W. Bequette, *Process Control: Modeling, Design and Simulation*, Prentice Hall PTR (2002).
13. D. B. Neumann and H. W. Rose, "Improvement of recorded holographic fringes by feedback control," *Appl. Opt.* **6**, 1097–1104 (1967).
14. S. P. McGrew, "An inexpensive fringe stabilizer for long exposure holography," in *Int. Symp. on Display Holography*, Vol. **1**, pp. 189–193, Lake Forest College, Lake Forest, FL (1982).
15. J. G. Ziegler and N. B. Nichols, "Optimum settings for automatic controllers," *Trans. ASME* **64**, 759–765 (1942).
16. C. M. Vest, *Holographic Interferometry*, Chap. 1, pp. 1–64, John Wiley and Sons, Inc., New York (1979).
17. P. Kromer, R. Robinett, R. Bengtson, and C. Hays, "PC-based digital lock-in detection of small signals in the presence of noise," AAPT Apparatus Competition, http://mrflip.com/papers/LIA/AAPTPaper/AAPTPaper.PDF (1999).
18. Newport Corp., *Laser Beam Stabilization Modules*, pp. 397–398.
19. K. Buse, A. Adibi, and D. Psaltis, "Non-volatile holographic recording in doubly doped lithium niobate crystals," *Nature (London)* **393**, 665–668 (1998).
20. J. N. Butters, *Holography and its Technology*, Chap. **6**, pp. 93–121, Peter Peregrinus Ltd, Cambridge (1971).

George H. Cadena received his BS degree in electrical engineering from Georgia Institute of Technology in 2004. He was enrolled in a two-year Christian Bible college called the Full Time Training in Anaheim (FTTA). He started his PhD in the School of Electrical Engineering, California Institute of Technology, in fall 2006. For his undergraduate research, he received ECE Outstanding Undergraduate Research Award from School of Electrical and Computer Engineering, Georgia Institute of Technology, in April 2005. His research interests are holography, interferometry, and biophotonics.

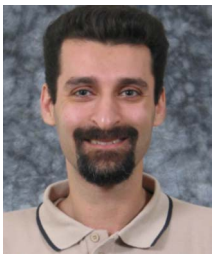

Omid Momtahan obtained a BS degree in electrical engineering from the Shiraz University in 1996, ranking first among his graduating class. He was with the Electrical Engineering Department of Sharif University of Technology from 1996, obtaining a MS degree in 1998. Currently, he is a PhD student at the School of Electrical and Computer Engineering, Georgia Institute of Technology. He is the recipient of the Outstanding Young Researcher Award, from Optics in the Southeast Conference, Atlanta, GA, in October 2005, and the Electrical and Computer Engineering Graduate Research Assistant Excellence Award from the School of Electrical and Computer Engineering, Georgia Institute of Technology, in April 2005. His technical interests are volume holographic memories, optical spectroscopy, biosensors, biophotonics, optical communications, and wireless communications.

Ali Adibi received the BSEE degree from Shiraz University, Shiraz, Iran, in 1990, and the MSEE and PhD degrees from Georgia Institute of Technology, Atlanta, in 1994 and California Institute of Technology, Pasadena, in 2000, respectively. His PhD research resulted in a breakthrough in persistent holographic storage in photorefractive crystals. He worked as a postdoctoral scholar at California Institute of Technology from 1999 to 2000 and joined Georgia Tech in 2000, where he is currently an associate professor. His research interests include holographic data storage; holographic optical elements for optical communications; 3-D optical pattern recognition; design, characterization, and applications of photonic crystals for chip-scale wavelength-division multiplexing and biosensors; and optical communication and networking.